Computation of Two-Dimensional, Transonic, Chemically Reacting Nonequilibrium Flow in a Rocket Nozzle

By

Kazuhiro NAKAHASHI*

(February 1, 1983)

Summary: A time-dependent, semi-implicit scheme is developed for solving the equations governing two-dimensional, chemically reacting nonequilibrium flow inside rocket nozzles. Subsonic and transonic flowfields of the nozzle entrance and throat region can be analyzed using this computational scheme. All equations of motion are solved simultaneously at each grid point by treating the time derivatives implicitly, in order to make the scheme stable with respect to the chemical rates. By evaluating spatial derivative terms explicitly, the scheme is made simple and has the advantage that only a relatively small computer storage is required. Results are presented at first for a nonreacting flow inside the JPL nozzle in order to illustrate the proposed scheme's validity by comparing with the experimental data and the result of the Cline's scheme. Then the nozzle flowfield of a hydrogen-oxygen rocket engine is analyzed. A computational result of C-H-O-N system (nitrogen tetroxide and a blend of 50 percent hydrazine and 50 percent unsymmetrical dimethyl hydrazine) is also presented.

Nomenclature

a_f = frozen speed of sound, $\sqrt{\gamma_f p/\rho}$
C_i = spacies i mass fraction
C_p = specific heat at constant pressure
h = enthalpy
h_i = enthalpy of species i
h_i^0 = energy of formation of species i
Ns = number of chemical species
p = pressure
$\bar{R}$ = uneversal gas constant
T = temperature
t = time
u = axial velocity component
v = radial velocity component
W_i = molecular weight of species i
x = axial coordinate
y = radial coordinate
y_c = center body coordinate
y_w = nozzle wall coordinate
γ_f = ratio of frozen specific heats
ε = geometric index
ζ = transformed axial coordinate
η = transformed radial coordinate
ρ = density
τ = transformed time
ψ_k = energy equation source term
ω_i = species i production rate

Superscripts

n = time step

1. Introduction

Performance prediction for a rocket propulsion system requires a detailed analysis of the flow through the exhaust nozzle. The need for high accuracy has become

* National Aerospace Laboratory

increasingly important because of the higher chamber pressure of today's engines. Tomorrow's adbanced engines, such as plug nozzle engines and dual nozzle engines (Figure 1 [1]), also require the aerodynamic analysis in order to design the optimum nozzle contour and the nozzle cooling system. However, the calculation of a two-dimensional flow with finite-rate chemical reactions is very time consuming, because of a large number of chemical species taking part in a problem, and of the stiffness of chemical relaxation equations in a near equilibrium flow region. The stiffness of equations makes it impractical to use a standard explicit integration method.

The analysis of the nozzle flowfield can be divided into two parts; the analysis of the subsonic and transonic flows in the nozzle entrance and throat regions, and the analysis of the supersonic flow in the nozzle divergence. The effects of finite-rate kinetics must be included in both parts of the analysis. For the supersonic fiowfield, a method-of-characteristics technique [2] or a space-marching finite-difference scheme [3] are proposed. On the other hand the subsonic-transonic flow regions have been solved under certain approximations, such as a quasi-one-dimensional kinetic flow [4] or a two-dimensional isentropic flow [5]–[10]. One-dimensional approximation is usefull for the computation of a conventional rocket nozzle and has been used in the rocket nozzle performance prediction code [2]. However this approach is limited in their applicability. It produces poor results when applied to the flowfields of the nozzle entrance region having a very steep wall gradient or of an unconventional rocket nozzle. The time-dependent method under the assumption of isentropic flow has also less meaning if a rocket nezzle flowfield, where the finite-rate kinetics effects are particularly important, is considered. Thus the subject research has heen directed to build up a computational method for

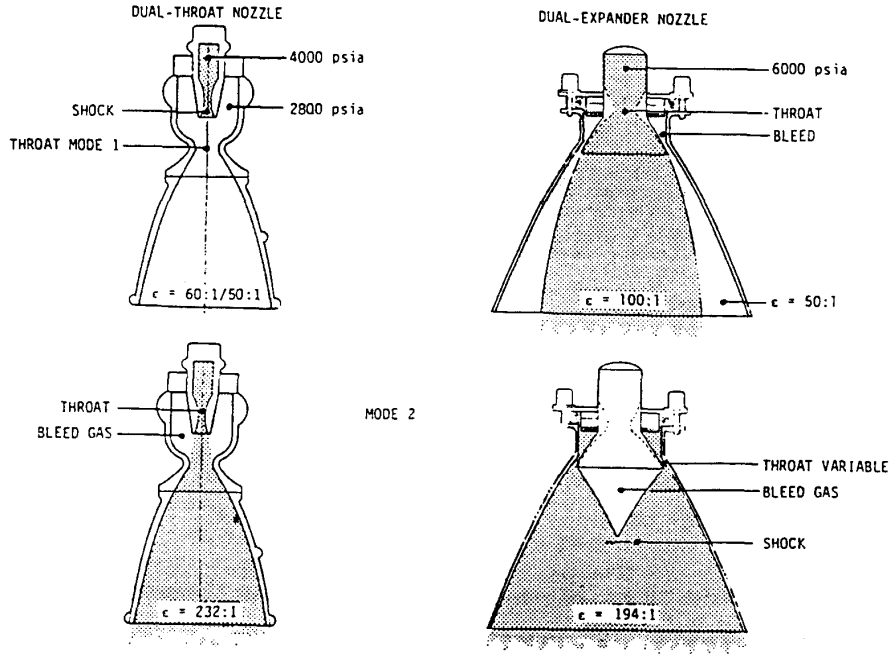

Fig. 1. Dual nozzle engine [1].

the two-dimensional chemically reacting flow in the rocket nozzle throat region.

Before we discuss the proposed scheme, it is worth to review the time-dependent techniques [5]–[10] which were applied to the nenreacting nozzle flow problems. In solving the internal flow problem, treatments of the inlet and wall boundary directry affect the overall computational stability and accuracy. Wehofer and Moger [6], Laval [7], and Brown and Ozcan [9] used an extrapolation technique to compute the wall mesh points, and Serra [8] used a reflection technique. However, a reference-plane characteristic method used by Migdal, et al. [5] and Cline [10] may be the most reliable one. Cline also successfully applied this characteristic method to compute the inlet mesh points. For the treatments of the interior mesh points, Cline compared his scheme to the other ones and concluded that the MacCormack's explicit scheme with the equations of motion in non-conservation form was the most efficient one. Chang [11] also uses the MacCormack's scheme in solving the gas-particle, two-phase inviscid flow inside nozzles.

All methods mentioned above are restricted to nonreacting gas flows using explicit integration schemes, and can not be applied to the reacting gas flows because of the stiffness. In order to cope with this difficulty, Kee and Dwyer [12] recommended to apply a Beam-Warming type fully implicit scheme to combustion problems. However, this fully implicit scheme needs a very large computer storage for a problem where a large number of chemical species takes part in. Stites and Hoffman [13] proposed an unsteady, asymptotically consistent technique. In their scheme, the species continuity equations are integrated by an implicit method along streamlines and the fluid dynamic equations are integrated using MacCormack's explicit method. However, there may be yet room for improvement in the computational efficiency.

In this paper, the semi-implicit scheme, which is proposed by Nakahashi [3] for the supersonic reacting flow, is extended to the subsonic-transonic flowfield with the time-dependent technique. In order to cope with the stiffness of the reacting flow problem, it is most important that all equations are solved in fully coupled form. This simultaneous solution procedure can be made by evaluating the time derivatives implicitly. On the other hand, the fully implicit scheme requires an excessive computer storage. For example, the number of unknowns for a rocket nozzle flow problem with hydrogen-oxygen propellant is at least ten, and for hydrocarbon propellant, twenty or more. These numbers of unknowns make it impossible to use a fully implicit scheme. In the proposed scheme, the computer storage is saved by evaluating spatial derivative terms explicitly. A disadvantage of this explicit treatment of spatial derivative terms is the time step size restriction by the CFL condition. However, the step size can not be so large even if the fully implicit scheme is employed, because of the chemical stiffness. With the consideration of the arithmetic operational counts [3], the proposed scheme's computational efficiency may be better than that of the fully implicit one.

2. Conservation Equations

The basic assumptions made in the derivation of equations for a nozzle flow of reacting gas mixtures are as follows.

(a) The gas is inviscid.
(b) Each component of the gas in a perfect gas.
(c) The flow is assumed to be everywhere in instantaneous translational, rotational, and vibrational equilibrium.

Under these assumptions, the conservation equations for two-dimensional planar flow ($\varepsilon=0$) or axisymmetric flow ($\varepsilon=1$) are given by

$$\rho_t+u\rho_x+v\rho_y+\rho(u_x+v_y+\varepsilon v/y)=0 \tag{1}$$
$$u_t+uu_x+vu_y+p_x/\rho=0 \tag{2}$$
$$v_t+uv_x+vv_y+p_y/\rho=0 \tag{3}$$
$$p_t+up_x+vp_y-a_f^2(\rho_t+u\rho_x+v\rho_y)=\psi_k \tag{4}$$
$$C_{i_t}+uC_{i_x}+vC_{i_y}=\omega_i/\rho, \qquad i=1, \cdots, Ns \tag{5}$$

and

$$p=\rho RT \tag{6}$$
$$\psi_k=\sum_{i=1}^{Ns}\left[\gamma_f\left(\frac{\bar{R}}{W_i}\right)T-(\gamma_f-1)h_i\right]\omega_i \tag{7}$$

The subscripts in these equations denote partial differentiation. The system enthalpy and gas constant are

$$h=\sum_{i=1}^{Ns}C_ih_i \quad \text{where} \quad h_i=\int_{T_0}^{T}C_{pi}\,dT+h_i^0 \tag{8}$$
$$R=\sum_{i=1}^{Ns}C_i\left(\frac{\bar{R}}{W_i}\right) \tag{9}$$

Since the interior points in this analysis are to be treated by a fixed grid technique, it is convenient to transform the physical (x, y, t) plane to a rectangular (ζ, η, τ) plane, as illustrated in Figure 2. The following coordinate transformation is employed.

$$\left.\begin{aligned}\zeta&=x\\ \eta&=\frac{y-y_c(x)}{y_w(x)-y_c(x)}\\ \tau&=t\end{aligned}\right\} \tag{10}$$

Applying this transformation to Eqs. (1) to (5) yields the final form of governing equations as

$$\frac{\partial z_i}{\partial \tau}=f_i, \qquad i=1, \cdots, Ns+4 \tag{11}$$

where z_i represent the velocity components (u, v), pressure p, density ρ, and species mass fraction C_j, $j=1, \cdots, Ns$, respectively. f_i is the function of these unknowns.

$$f_1=-[uu_\zeta+\bar{v}u_\eta+p_\zeta/\rho+\alpha p_\eta/\rho] \tag{12}$$

$$f_2=-[uv_\zeta+\bar{v}v_\eta+\beta p_\eta/\rho] \tag{13}$$

$$f_3=-[up_\zeta+\bar{v}p_\eta+\rho a_f^2(u_\zeta+\alpha u_\eta+\beta v_\eta+\varepsilon v/\bar{\eta})]+\psi_k \tag{14}$$

$$f_4=-[u\rho_\zeta+\bar{v}\rho_\eta+\rho(u_\zeta+\alpha u_\eta+\beta v_\eta+\varepsilon v/\bar{\eta})] \tag{15}$$

$$f_{4+i}=\omega_i/\rho-[uC_{i\zeta}+\bar{v}C_{i\eta}] \tag{16}$$

where

$$\left.\begin{aligned} &\alpha=-\beta(dy_c/dx)-\eta\beta(dy_w/dx), && \beta=1/(y_w-y_c)\\ &\bar{v}=\alpha u+\beta v, && \bar{\eta}=y_c+\eta/\beta \end{aligned}\right\} \tag{17}$$

The net species production rate, ω_i, appearing in Eqs. (5) and (7) is determined by the method described below.

A chemical reaction can be written in terms of its stoichiometric coefficients (ν_{ij} and ν'_{ij}) as

$$\sum_{i=1}\nu_{ij}Z_i \rightleftarrows \sum_{i=1}\nu'_{ij}Z_i \tag{18}$$

where Z_i represents the i-th chemical species name and j represents the j-th reaction.

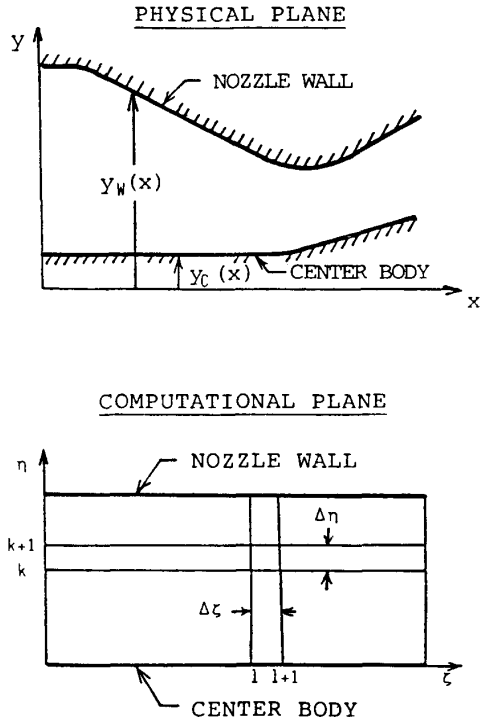

Fig. 2. Coordinate systems.

Given a system of chemical reactions, the net species production rate ω_i for each species is calculated from

$$\omega_i = W_i \sum_{j=1} \rho^{\sum_{l=1} \nu_{lj}} (\nu'_{ij} - \nu_{ij}) X_j$$

where

$$X_j = \left[k_{fj} \prod_{i=1} \left(\frac{C_i}{W_i} \right)^{\nu_{ij}} - k_{bj} \rho^{\sum_{l=1} (\nu'_{lj} - \nu_{lj})} \prod_{i=1} \left(\frac{C_i}{W_i} \right)^{\nu'_{ij}} \right] M_j. \tag{20}$$

The reverse reaction rate, k_{bj}, in the above equation is represented in the Arrhenius form

$$k_{bj} = a_j T^{-n_j} e^{(-b_j/\bar{R}T)}. \tag{21}$$

The forward reaction rate, k_{fj}, is calculated by using the equilibrium constant, K_j, as

$$k_{fj} = k_{bj} K_j \tag{22}$$

and

$$K_j = e^{-\Delta F_j/\bar{R}T} (\bar{R}T^{-\sum_{l=1} (\nu'_{lj} - \nu_{lj})}) \tag{23}$$

where ΔF_j is a change in free energy during the reaction process.

$$\Delta F_j = \sum_{i=1} F_i \nu'_{ij} - \sum_{i=1} F_i \nu_{ij}. \tag{24}$$

The term M_j is provided so that the reaction rate can be modified for reactions involving a third body, namely

$$\left.\begin{aligned} M_j &= \sum_{i=1} m_{ji} \left(\frac{C_i}{W_i} \right) \quad \text{for reactions requiring a third body} \\ M_j &= 1 \quad \text{for all other reactions} \end{aligned}\right\} \tag{25}$$

where the constants m_{ji} are specified.

3. Finite-Difference Scheme

When a second-order implicit difference approximation is applied to the time

$$\Delta z_i^{(n+1)} = \tfrac{1}{2} \Delta\tau^{(n+1)} [f_i^{(n)} + f_i^{(n+1)}] + O(\Delta\tau^3), \qquad i = 1, \cdots, Ns+4 \tag{26}$$

where

$$\Delta z_i^{(n+1)} = z_i^{(n+1)} - z_i^{(n)}, \qquad \Delta\tau^{(n+1)} = \tau^{(n+1)} - \tau^{(n)} \tag{27}$$

and the superscript n refers to time steps.

As the nonlinear function $f_i^{(n+1)}$ includes the unknowns $z_j^{(n+1)}$, $j = 1, \cdots, Ns+4$ implicitly, we need to consider the linearization of $f_i^{(n+1)}$ in $z_j^{(n+1)}$ so as to make

the scheme noniterative. This linearization can be obtained using a local Taylor expansion, regarding f_i as a function of z_j, z_{j_ζ}, z_{j_η}, $j=1, \cdots, Ns+4$.

$$f_i^{(n+1)}=f_i^{(n)}+\sum_{j=1}^{Ns+4}[A_{ij}^{(n)}\Delta z_j^{(n+1)}+B_{ij}^{(n)}\Delta z_{j_\zeta}^{(n+1)}+C_{ij}^{(n)}\Delta z_{j_\eta}^{(n+1)}]+O(\Delta\tau^2) \tag{28}$$

where

$$A_{ij}=\partial f_i/\partial z_j, \qquad B_{ij}=\partial f_i/\partial z_{j_\zeta}, \qquad C_{ij}=\partial f_i/\partial z_{j_\eta} \tag{29}$$

In this linearization procedure, however, the derivative terms with respect to ζ and η, $\Delta z_{j_\zeta}^{(n+1)}$ and $\Delta z_{j_\eta}^{(n+1)}$, require an additional consideration. There are two methods to evaluate them. One of the methods is an implicit evaluation method and the other is an explicit one. In the proposed scheme, these terms are evaluated by the explicit one in order to save the computer storage. Namely,

$$\begin{aligned}\Delta z_{j_\zeta}^{(n+1)}&=z_{j_{\zeta\tau}}^{(n)}\Delta\tau^{(n+1)}+O(\Delta\tau^2)=f_{j_\zeta}^{(n)}\Delta\tau^{(n+1)}+O(\Delta\tau^2)\\ \Delta z_{j_\eta}^{(n+1)}&=z_{j_{\eta\tau}}^{(n)}\Delta\tau^{(n+1)}+O(\Delta\tau^2)=f_{j_\eta}^{(n)}\Delta\tau^{(n+1)}+O(\Delta\tau^2)\end{aligned} \tag{30}$$

Substituting Eqs. (30) and (28) into Eq. (26), and neglecting the terms $O(\Delta\tau^3)$, we get a following linear algebraic equation system of order $Ns+4$.

$$\Delta z_i^{(n+1)}-\frac{\Delta\tau^{(n+1)}}{2}\sum_{j=1}^{Ns+4}A_{ij}^{(n)}\Delta z_j^{(n+1)}=\frac{\Delta\tau^{(n+1)}}{2}[f_i^{(n)}+g_i^{(n)}] \tag{31}$$

where

$$g_i^{(n)}=f_i^{(n)}+\Delta\tau^{(n+1)}\sum_{j=1}^{Ns+4}[B_{ij}^{(n)}f_{j_\zeta}^{(n)}+C_{ij}^{(n)}f_{j_\eta}^{(n)}] \tag{32}$$

Thus the flowfield solution can be obtained by solving the above set of simultaneous equations, Eq. (31), which is constructed at each grid point.

However, we meet with another difficulty of the static numerical instability if a centered difference scheme is employed to approximate spatial derivatives included in $A_{ij}^{(n)}$, $f_i^{(n)}$, and $g_i^{(n)}$ of Eq. (31). In order to get over this numerical difficulty, a noncentered difference approximation was employed to evaluate these spatial derivatives. Namely, the spatial derivatives included in $f_i^{(n)}$ of Eq. (31), which is equivalent to $f_i^{(n)}$ of Eq. (26), are approximated by the two-point backward difference and those in $A_{ij}^{(n)}$ and $g_i^{(n)}$ in Eq. (31), which are derived from $f_i^{(n+1)}$ in Eq. (26), by the forward difference. With this noncentered scheme, the proposed scheme becomes stable and has a reasonable accuracy.

By evaluating $\Delta z_{j_\zeta}^{(n+1)}$ and $\Delta z_{j_\eta}^{(n+1)}$ in Eq. (28) explicitly in the proposed scheme, the time step size $\Delta t^{(n+1)}$ is restricted by the CFL condition. A fully implicit method whose step size is not retricted by the CFL condition may be possible if the above terms is evaluated implicitly. However this fully implicit method was not employed in the present study, because it requires an excessive memory size.

4. Boundary and Initial Conditions

The inlet mesh points are computed using a constant-η, reference-plane characteristic method. The characteristic and compatibility equations are

along $$d\zeta=(u-a_f)d\tau \tag{33}$$

$$dp-\rho a_f du=-\bar{v}p_\eta-\rho a_f^2\left(\alpha u_\eta+\beta v_\eta+\frac{\varepsilon v}{\eta}\right)+\rho a_f\left(\bar{v}u_\eta+\frac{\alpha p_\eta}{\rho}\right)+\psi_k \tag{34}$$

Since there are $Ns+4$ unknowns at the inlet (u, v, p, ρ, and C_j, $j=1, \cdots, Ns$) and only one compatibility equation, $Ns+3$ additional conditions must be specified. We specify the distridutions of the species mass fractions, C_j, and the inlet flow angle, θ_i ($=\tan^{-1}v/u$), on the entrance plane. The remaining unknowns are determined by Eqs. (33) and (34) as well as the total enthalpy $H_0=h+(u^2+v^2)/2$, total pressure p_0, which are also specified at the inlet plane.

The well points are computed using a constant-ζ reference-plane characteristic method. Following characteristic are compatibility equations are derived from Eqs. (1) to (5).

(i) along $\lambda=d\eta/d\tau=\bar{v}$ (35)

$$\beta du-\alpha dv=(\beta\phi_2-\alpha\phi_3)d\tau \tag{36}$$

$$dp-a_f^2 d\rho=\phi_4 d\tau \tag{37}$$

$$dC_i=\phi_{i+i}d\tau \tag{38}$$

(ii) along $\lambda=d\eta/d\tau=\bar{v}+a_f\alpha^*$ (39)

$$dp+\frac{\rho a_f}{\alpha^*}(\alpha du+\beta dv)=\left[\phi_4+a_f^2\phi_1+\frac{\rho a_f}{\alpha^*}(\alpha\phi_2+\beta\phi_3)\right]d\tau \tag{40}$$

where

$$\left.\begin{aligned}&\phi_1=-u\rho_\zeta-\rho(u_\zeta+\varepsilon v/\bar{\eta}), && \phi_2=-uu_\zeta-p_\zeta/\rho\\ &\phi_3=-uv_\zeta, && \phi_4=-up_\zeta+a_f^2 u\rho_\zeta+\psi_k\\ &\phi_{4+i}=-uC_{i\zeta}+\sigma_i/\rho, && \alpha^*=\sqrt{\alpha^2+\beta^2}\end{aligned}\right\} \tag{41}$$

In addition to Eqs. (35) to (40), flow tangency at the wall is required. This is

$$v=u\tan\theta_{\text{wall}} \tag{42}$$

Above equations can be solved by an iterative scheme for an isentropic flow. However for the chemically reacting flow, all equations should be solved simultaneously. This coupled solution procedure employed in the proposed scheme are as follows. First, all equations are approximated to the difference form between points 1–5 and 4–5 in Figure 3. Then the nonlinear functions appeared in the difference equations are linearized by the method similar to that for the interior points. This procedure results a set of simultaneous equations for the unknowns u, p, ρ, C_j, $j=1, \cdots, Ns$. Details of the proposed scheme for the wall boundary

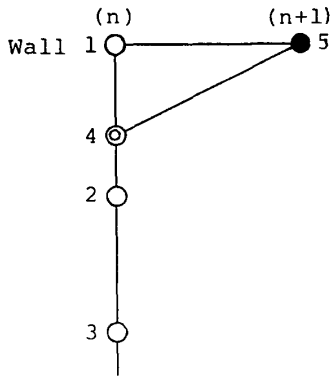

Fig. 3. Wall boundary treatment

can be seen in Ref. (3) which describes the scheme for supersonic flow fields.

Exit boundary points are computed by linear extrapolation from the first and second adjacent interior points, assuming the supersonic exit.

Initial conditions for starting the solution procedure are given using a full one-dimensional finite-rate kinetic solution (ODK). Preceding to the ODK solution, combustion chamber conditions are determined using the equilibrium composition computational program (ODE) [14].

The time step size is given by the CFL criterion to two-dimensional, unsteady flow.

$$\Delta\tau=\mathrm{Min}\left\{\frac{C}{\sqrt{8}}\sqrt{\Delta\zeta^2+(\Delta\eta/\beta)^2}/[\sqrt{u^2+v^2}+a_f]\right\} \tag{43}$$

where C is a constant and $0<C\leq 1$.

5. Computational Results

Nonreactive Gas Flow

In order to test the validity of the proposed scheme, a nonreactive gas flow inside the JPL axisymmetric nozzle [15] with 45 deg entrance and 15 deg exit straight wall tangent to a circular throat (with ratio of throat radius of curvature to throat height=0.625) was calculated. Figure 4 shows a comparison of the computed Mach number contours inside the nozzle with the experimental data. The Mach number contours of the proposed semi-implicit scheme are also compared with those obtained by Cline's scheme [10], in which the MacCormack's explicit method is used, as illustrated in Figure 5. These comparisons show good agreements of the proposed scheme's results with those of experimental and the Cline's scheme.

H–O System

For the practical rocket nozzle flow, Figure 6 shows computed Mach number contours inside a LO_2/LH_2 engine whose firing test has been conducted at National Aerospace Labolatory [16]. In the calculation, eight chemical reactions with six chemical species (H, H_2, H_2O, O, O_2, OH) are considered as shown Table 1.

Figure 7 shows the computed axial pressure distributions along the nozzle wall and the center line. This figure also shows the one-dimensional kinetic (ODK)

result, demonstrating the deficiency of the ODK result near the throat region. The pressure distribution along the nozzle wall in the throat region has much importance to a critical design of the nozzle wall cooling system.

Radial pressure and Mach number distributions at the throat plane are shown in Figure 8, comparing with an analytical solution of Kliegel and Levine [17]. In the calculation of the analytical solution, the ratio of constant specific heats is derived from an average expansion coefficient which is computed using ODK results as

$$\bar{\gamma}=\ln(p_2/p_1)/\ln(\rho_2/\rho_1)$$

where the subscripts 1 and 2 refer to the values of throat entrance and throat exit point, respectively. As shown in this figure, the analytical solution is very

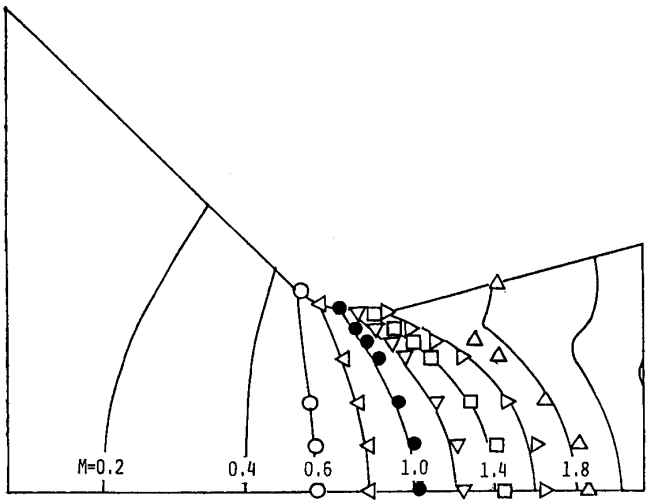

Fig. 4. Mach number contours for JPL nozzle (nonreactive gas flow).

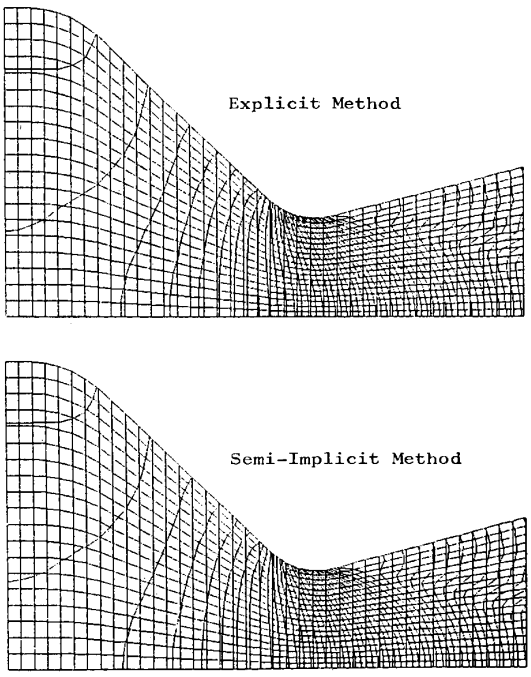

Fig. 5. Comparison of Mach number contours of the proposed scheme with Cline's scheme (nonreactive gas flow inside JPL nozzle).

Table 1. Reaction mechanism for H–O system

No.	reaction	reaction rate
1	$O_2 + M = O + O + M$	$k_f = 1.2 \times 10^{17}\ T^{-1}$
2	$H_2 + M = H + H + M$	$k_f = 6.4 \times 10^{17}\ T^{-1}$
3	$H_2O + M = H + OH + M$	$k_f = 7.5 \times 10^{23}\ T^{-2.6}$
4	$OH + M = O + H + M$	$k_f = 4.0 \times 10^{18}\ T^{-1}$
5	$H + H_2O = H_2 + OH$	$k_f = 2.19 \times 10^{13} \exp(-5150/RT)$
6	$O + H_2O = OH + OH$	$k_f = 5.75 \times 10^{12} \exp(-780/RT)$
7	$O + H_2 = H + OH$	$k_f = 7.33 \times 10^{12} \exp(-7300/RT)$
8	$H + O_2 = O + OH$	$k_f = 1.3 \times 10^{13}$

usefull if it is used under limitations that Mach number is close to one and the nozzle wall has a circular configuration. However, this simplified method becomes less accurate when a nozzle contour with a very small throat radius of curvature or a very steep wall gradient in the entrance region is to be analyzed. The proposed numerical technique is well suited for application to these different nozzle geometric configurations, and to the unconventional nozzles.

C–H–O–N System

A computational result of the C–H–O–N system is shown is Figure 9. This

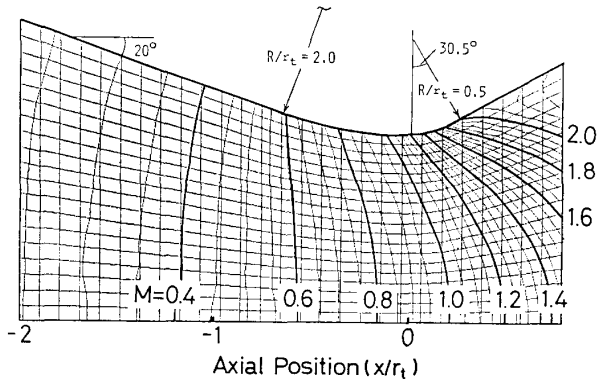

Fig. 6. Mach number contours inside a LO_2/LH_2 engine nozzle (throat radius r_t=0.014 m).

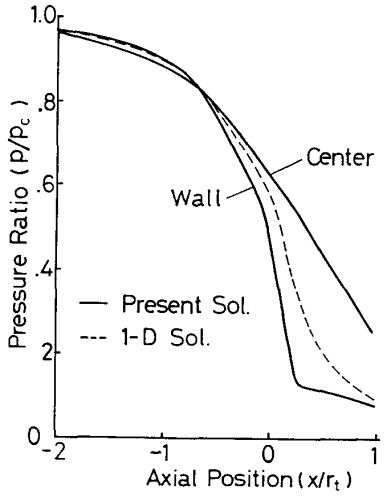

Fig. 7. Axial pressure profiles.

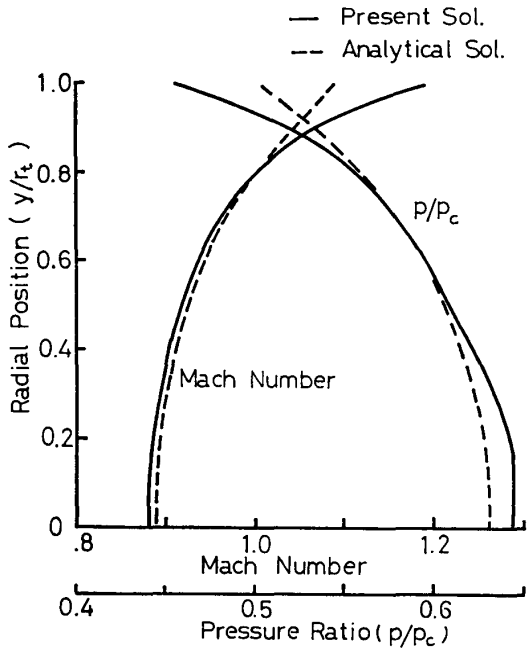

Fig. 8. Radial pressure and March number profiles at throat.

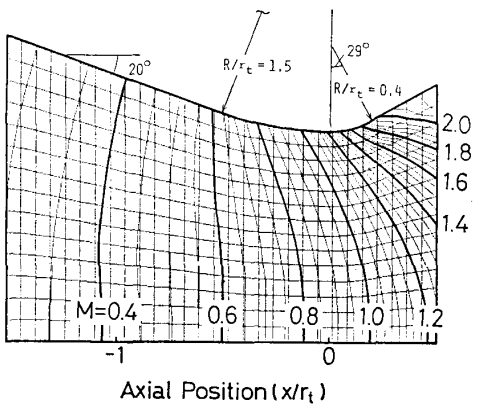

Fig. 9. Mach number contours inside LE-3 engine nozzle (throat radius r_t= 0.0925 m).

Table 2. Reaction mechanism for C–H–O–N system.

No.	reaction	reaction rate
1	$H + OH + M = H_2O + M$	$k_f = 7.5 \times 10^{23} T^{-2.6}$
2	$O + H + M = OH + M$	$k_f = 4.0 \times 10^{18} T^{-1}$
3	$O + O + M = O_2 + M$	$k_f = 1.2 \times 10^{17} T^{-1}$
4	$H + H + M = H_2 + M$	$k_f = 6.4 \times 10^{17} T^{-1}$
5	$CO_2 + M = O + CO + M$	$k_f = 2.7 \times 10^{32} T^{-4.5} \exp(-127555/RT)$
6	$C + O + M = CO + M$	$k_f = 3.0 \times 10^{16} T^{-.5}$
7	$N + N + M = N_2 + M$	$k_f = 1.0 \times 10^{18} T^{-1}$
8	$N + O + M = NO + M$	$k_f = 6.4 \times 10^{16} T^{-.5}$
9	$H_2 + OH = H + H_2O$	$k_f = 2.19 \times 10^{13} \exp(-5150/RT)$
10	$OH + OH = O + H_2O$	$k_f = 5.75 \times 10^{12} \exp(-780/RT)$
11	$H + OH = O + H_2$	$k_f = 7.33 \times 10^{12} \exp(-7300/RT)$
12	$O + OH = H + O_2$	$k_f = 1.3 \times 10^{13}$
13	$OH + CO = H + CO_2$	$k_f = 5.6 \times 10^{11} \exp(-1080/RT)$
14	$O_2 + CO = O + CO_2$	$k_f = 8.85 \times 10^{9} T^{.656} \exp(-45920/RT)$
15	$OH + OH = H_2 + O_2$	$k_f = 1.41 \times 10^{13} T^{-.015} \exp(-49264/RT)$
16	$NO + NO = N_2 + O_2$	$k_f = 1.0 \times 10^{13} \exp(-79490/RT)$
17	$N + NO = O + N_2$	$k_f = 3.1 \times 10^{13} \exp(-334/RT)$
18	$N + O_2 = O + NO$	$k_f = 6.43 \times 10^{9} T^{1} \exp(-6250/RT)$
19	$CO_2 + C = CO + CO$	$k_f = 1.1 \times 10^{11} T^{.5} \exp(-6995/RT)$
20	$C + OH = CO + H$	$k_f = 5.3 \times 10^{11} T^{.5} \exp(-5628/RT)$
21	$C + NO = CO + N$	$k_f = 5.3 \times 10^{11} T^{.5} \exp(-8303/RT)$
22	$CO_2 + N = CO + NO$	$k_f = 1.1 \times 10^{11} T^{.5} \exp(-59618/RT)$
23	$C + O_2 = CO + O$	$k_f = 5.3 \times 10^{11} T^{.5} \exp(-6552/RT)$
24	$N + OH = NO + H$	$k_f = 5.3 \times 10^{11} T^{.5} \exp(-5628/RT)$

nozzle (LE-3 engine [18]) was used as the second stage engine of the N–1 rocket of Japan. Nitrogen tetroxide (N_2O_4) and a blend of 50 percent hydrazine and unsymmetrical dimethyl hydrazine (50–50 fuel blend) is used as the rocket propellant. As shown in Table 2, 24 reactions of 12 chemical species (H, H_2, H_2O, O, O_2, OH, C, CO, CO_2, N, N_2, NO) are taken into account.

Computational Time

Computational time is highly problem dependent. It is especially sensitive to the number of chemical species and reactions in the problem model. This is because a set of simultaneous equations of order $Ns+4$ is solved at every each grid point and the arithmetic operational count of the Gauss-elimination method for simultaneous equations is proportionate to $(Ns+4)^3$. For the cases mensioned above, the solutions were obtained in CUP time ranging three to four hours for H–O system and fifteen to twenty hours for C–H–O–N system, using a FACOM M160F computer which is a middle level computational speed computer. These times will be reduced by one-tenth or more if a modern high-speed computer is used.

6. Conclusions

The primary contribution of this research is the development of a semi-implicit integration scheme for two-dimensional subsonic nozzle flows including the effects of finite-rate chemical kinetics. The main features of the proposed method are as follows. All equations are solved simultaneously at each grid point by treating time derivatives implicitly, which make the scheme stable with respect to the chemical rates. The spatial derivative terms are evaluated explicitly, so that the required computer storage is greatly reduced compared to the fully implicit method.

References

[1] O'Brien, C. J.: Dual-Nozzle Design Update, AIAA-82-1154, 1982.
[2] Nickerson, G. R., Coats, D. E., and Bartz, J. L.: The Two-Dimensional Kinetic (TDK) Reference Computer Program: Engineering and Programing Manual, NASA-CR-152999, 1977.
[3] Nakahashi, K.: An Implicit Finite Difference Method for Chemical Nonequilibrium Flow Through an Axisymmetric Supersonic Nozzle, Proc. of 8th ICNMFD, Aachen, 1982, or Trans. Japan Soc. Aero. Space Sci., Vol. 25, No, 69, pp. 160-173, 1982.
[4] Bittker, D. A. and Scullin, V. J.: General Chemical Kinetics Computer Program for Static and Flow Reactions, with Application to Combustion and Shock-Tube Kinetics, NASA TN D-6586, 1972.
[5] Migdal, D., Klein, K., and Moretti, G.: Time-Dependent Calculations for Transonic Nozzle Flow, AIAA J., Vol. 7, No. 2, pp. 372-374, 1969.
[6] Wehofer, S. and Moger, W. C.: Transonic Flow in Conical Convergent and Convergent-Divergent Nozzles with Nonuniform Inlet Conditions, AIAA-70-635, 1970.
[7] Lavel, P.: Time-Dependent Calculation Method for Transonic Nozzle Flows, Proc. of 2nd ICNMFD, Lecture Notes in Physics, Vol. 8, pp. 187-192, 1971.
[8] Serra, R. A.: Determination of Internal Gas Flows by a Transient Numerical Technique, AIAA J., Vol. 10, No. 5, pp. 603-611, 1972.
[9] Brown, E. F. and Ozcan, H. M.: A Time-Dependent Solution of Mixed Flow Through Convergent Nozzles, AIAA-72-680, 1972.
[10] Cline, M. C.: Computation of Steady Nozzle Flow by a Time-Dependent Method, AIAA J., Vol. 12, No. 4, pp. 419-420, 1974, or NASA TMX-71918.
[11] Chang, I-Shih: One- and Two-Phase Nozzle Flows, AIAA J., Vol. 18, No. 12, pp. 1455-1461, 1980.
[12] Kee, R. J. and Dwyer, H. A.: A Review of Stiffness and Implicit Finite Difference Methods in Combustion Modeling, SAND 79-8628, 1980.
[13] Stiles, R. J. and Foffman, J. D.: Analysis of Steady, Two-Dimensional, Chemically Reacting Nonequilibrium Flow by an Unsteady, Asymptotically Consistent Technique, AIAA-81-1432, 1981.
[14] Gorgon, S. and McBride, B. J.: Computer Program for Calculation of Complex Chemical Equilibrium Compositions, Rocket Performance, Incident and Reflected Shocks, and Chapman-Jouguet Detonations, NASA SP-273, 1971.
[15] Cuffel, R. F., Back, L. H., and Massier, P. F.: Transonic Flowfield in a Supersonic Nozzle with small Throat Radius of Curvatue, AIAA J., Vol. 7, No. 7, pp. 1364-1366, 1969.
[16] Miyajima, H., Nakahashi, K., Hirakoso, H., and Sogame, E.: Performance of a Low Thrust LO_2/LH_2 Engine with a 300: 1 Area Ratio Nozzle, to be appeared in AIAA Paper, 1983.
[17] Kliegel, J. R. and Levine, J. N.: Transonic Flow in Small Throat Radius of Curvature Nozzles, AIAA J., Vol. 7, No. 7, pp. 1375-1378, 1969.

[18] Otsuka, S. et al.: High Altitude Performance Tests of the N Rocket Second-Stage LE-3 Engine, Technical Memorandum of National Aerospace Laboratory, NAL TM-364, 1978 (in Japanese).